

## Basic development of a small balloon-mounted telemetry with its operation system

KONO, Hiroki<sup>1\*</sup> ; KAKINAMI, Yoshihiro<sup>1</sup> ; YAMAMOTO, Masa-yuki<sup>1</sup>

<sup>1</sup>Kochi Univ. of Tech

### 1. Introduction

In Japan, the high altitude balloon for scientific observation has been continuously launched by JAXA. The balloon has a possibility to reach 50 km altitude without severe environmental condition for onboard equipments, being operated with lower cost than sounding rockets, however, development of such large-scale scientific observing balloons by university laboratories is still difficult. Being coupled with rapid improvement of tiny semiconductor sensors recently, laboratory-basis balloon experiments using small weather balloons have been becoming easily in these years (e.g. Near Space Ventures, Inc., 2013).

Although the balloon is very small as its diameter of 6 feet, excluding its extra buoyancy and the weight of the balloon itself, it is expected that loading mass capacity of about 2 kg is remained for payloads to send it up to about 35 km. However, operation of such small balloons in Japan is not in general because precise prediction of a landing area of the payload is difficult, thus high-risk situation for balloon releases is still remained. In this study, we aim to achieve practical engineering experiments of weather balloons in Japan in order to operate laboratory level scientific observation within a university. Here we report an approach of developing many devices currently in progress.

### 2. Equipments development

We have been developing devices onboard a small tethered balloon for the future weather balloon release experiments. That is, one is a small-size and light-weight telemeter system of about 250 g that can be mounted on a commercially available balloon, while another is a ground station device that receives data from the telemeter. A combination of a wireless module, a GPS receiver, a barometer, a temperature and humidity meter, a camera, an accelerometer, an electronic compass, a power monitor sensor is mounted on the telemeter, and the measured values by each sensors can be transmitted in real time to the ground station device. Newly developed software for balloon operation can be run on a PC connected with the ground station device, it is possible to provide the operator the sensor information visualized in real time based on the position coordinates set on the ground station device using the software before the launch.

Real-time mapping of the balloon coordinates can be realized to rewrite a KML file to be input into the Google Earth continuously. In addition, azimuth and elevation of the balloon can be calculated by spherical trigonometry from obtained the GPS position. Providing these angles to a newly developed rotator to be mounted on a camera tripod, it is possible to track a small antenna automatically to the balloon direction continuously.

### 3. Result of the experiment

A tethered balloon experiment was performed for evaluating the developed telemeter system, however, there occurred unexpected issue in the communication distance. As a result, in the telemeter line, operating limit of the distance between the ground station and the telemeter is significantly shortened to approximately 110 m. It was almost different from our pre-experiment confirmation of a packet loss rate of 0% at 270 m distance in a preliminary experiment on ground.

Therefore, evaluation of the antenna rotator was carried out only at close range, i.e., in severe condition. It is because maximum elevation of the rotator was limited physically at 50 degrees or less, and there exists about 5 to 10 m error in the GPS positioning operated in the single receiver mode.

Nevertheless, it was possible to track the balloon continuously in a stable situation even in the shortened communication distance. In addition, the software and telemeter system worked as expected, the problem was not found in particular.

In this presentation, the data obtained by the tethered balloon experiment and detail of the developed equipments will be shown.

Keywords: Weather balloon, Tethered balloon, Stratosphere, Upper atmosphere, Telemeter, Embedded system

## Impacts of stratospheric sudden warming events in the mesosphere and lower thermosphere

WATANABE, Kumiko<sup>1\*</sup> ; TANAKA, Takashi<sup>1</sup> ; MIYOSHI, Yasunobu<sup>2</sup>

<sup>1</sup>Department of Earth and Planetary Sciences, Graduate School of Sciences, Kyushu University, <sup>2</sup>Department of Earth and Planetary Sciences, Faculty of Sciences, Kyushu University

Impacts of stratospheric sudden warming (SSW) events on the middle and upper atmosphere have been widely recognized. However, due to an insufficient number of global observations, SSW's effects on the general circulation in the mesosphere and lower thermosphere (MLT) are not well known. In this study, we investigate the short term variation of the temperature, zonal wind and meridional wind in the MLT region during SSW events using a general circulation model that contains the region from the troposphere to the thermosphere. We conducted GCM simulation with meteorological reanalysis data during the period from November 1, 2008 to March 31, 2010. Our results show that the temperature drop occurs in the Southern hemisphere, during SSW events. This means that SSW influences the general circulation in the summer hemisphere. Furthermore, it is found that the temperature in winter polar region in the lower thermosphere increases during SSW events. This is related to upward propagation of the planetary wave excited in the mesosphere.

Keywords: stratospheric sudden warming, mesosphere, lower thermosphere

## Vertical profiles of atmospheric temperature between upper troposphere and mesosphere obtained from Rayleigh/Raman lidar

NISHIYAMA, Takanori<sup>1\*</sup> ; NAKAMURA, Takuji<sup>1</sup> ; EJIRI, Mitsumu<sup>1</sup> ; ABO, Makoto<sup>2</sup> ; KAWAHARA, Taku d<sup>3</sup> ; TSUDA, Takuo<sup>1</sup> ; SUZUKI, Hidehiko<sup>4</sup> ; TSUTSUMI, Masaki<sup>1</sup> ; TOMIKAWA, Yoshihiro<sup>1</sup>

<sup>1</sup>National Institute of Polar Research, <sup>2</sup>Graduate School of System Design, Tokyo Metropolitan University, <sup>3</sup>Faculty of Engineering, Shinshu University, <sup>4</sup>Faculty of Science, Rikkyo University

Atmospheric gravity waves (AGWs) propagating upward from lower atmospheric sources play a dominant role in transporting and depositing energy and momentum from upper troposphere (UT) to lower mesosphere (LM). Particularly, in polar region, these effects of AGWs are well-known to strongly decelerate the polar night jet and drive large scale meridional circulation from the summer pole towards the winter pole. In addition, it is suggested that considerations of the realistic propagation property of AGWs may largely improve a significant bias of climate model. Therefore, investigation of the activity of AGWs between UT and LM based on continuous observational studies can be regarded as one of important issues.

The National Institute of Polar Research (NIPR) is leading a six year prioritized project of the Antarctic research observations since 2010. One of the sub-projects is entitled 'the global environmental change revealed through the Antarctic middle and upper atmosphere'. As a part of the sub-project, a Rayleigh/Raman lidar (RR lidar) was installed at Syowa, Antarctica (69S, 39E) in January, 2011. The operation has been conducted since February 2011 and the RR lidar has kept measuring temperature profiles continuously between approximately 10 and 80 km for almost 3 years.

The RR lidar system in Syowa can obtain photon count data for 4 channels simultaneously, and each data is recorded separately in binary format. The data from 3 channels, i.e., Raman (10-30km), Rayleigh-Low (20-65km), Rayleigh-High (30-80km), corresponding to different height ranges are used for estimations of temperature profiles from UT to LM. In order to estimate height continuous profiles of atmospheric temperature based on the 3 different channels, we are examining the following analysis methods. (1) The temperature for Rayleigh-High and Rayleigh-Low channels estimated by solving the lidar equation can be assigned to temperature at an initial height for the lidar equation in Rayleigh-Low and Raman channels, respectively. (2) The initial heights for the lidar equation can be determined automatically taking into account time and height dependent shot noises due to background luminosity. (3) The error propagations from the initial height to lower heights are evaluated by assigning artificial temperature offset ranging from -50 to 50 K.

The height continuous temperature profiles between UT and LM obtained from improved analysis methods would allow us to investigate important scientific issues such as temporal and height variabilities of potential energy per unit mass of AGWs and the relationship between occurrence of Polar Stratospheric Clouds and background atmospheric temperature. In this presentation, we will report the detail of the analysis methods and future perspectives including open data base of temperature profiles.

**Keywords:** Rayleigh/Raman lidar, Atmospheric temperature, Mesosphere, Stratosphere, Atmospheric Gravity Waves, Polar Stratospheric Clouds

## Tunable resonance scattering lidar system for Antarctic observation: Current status

TSUDA, Takuo<sup>1\*</sup> ; EJIRI, Mitsumu<sup>1</sup> ; NISHIYAMA, Takanori<sup>1</sup> ; ABO, Makoto<sup>2</sup> ; MATSUDA, Takashi<sup>1</sup> ; KAWAHARA, Takuya<sup>3</sup> ; NAKAMURA, Takuji<sup>1</sup>

<sup>1</sup>National Institute of Polar Research, <sup>2</sup>Graduate School of System Design, Tokyo Metropolitan University, <sup>3</sup>Faculty of Engineering, Shinshu University

We are developing a new resonance scattering lidar system to be installed at Syowa Station (69S, 39E) in Antarctica. For the new lidar system, we have employed a tunable alexandrite laser covering the resonance scattering wavelengths of two neutral species, which are atomic potassium (K, 770.11 nm) and atomic iron (Fe, 386.10 nm), and two ion species, which are calcium ion (Ca<sup>+</sup>, 393.48 nm) and aurorally excited nitrogen ion (N<sub>2</sub><sup>+</sup>, 390.30 nm, 391.08 nm). Thus the tunable resonance scattering lidar system will provide information on the mesosphere and lower thermosphere as well as the ionosphere. Using the tunable lidar and co-located other instruments, we will conduct a comprehensive ground-based observation of the low, middle, and upper atmosphere above Syowa Station. This unique observation is expected to make important contribution to studies on the atmospheric vertical coupling process and the neutral and charged particle interaction. In this presentation, we report current status of the tunable lidar system in development and test observations at National Institute of Polar Research in Tachikawa, Japan.

Keywords: Resonance scattering lidar, Antarctica, Syowa Station, K layer, Fe layer

## Doppler-free spectroscopy experiments for the Antarctic Potassium resonant lidar

KAWAHARA, Takuya<sup>1</sup> ; TSUDA, Takuo<sup>2\*</sup> ; NISHIYAMA, Takanori<sup>2</sup> ; EJIRI, Mitsumu<sup>2</sup> ; ABO, Makoto<sup>3</sup> ; NAKAMURA, Takuji<sup>2</sup>

<sup>1</sup>Faculty of Engineering, Shinshu University, <sup>2</sup>National Institute Polar Research, <sup>3</sup>System Design, Tokyo Metropolitan University

The National Institute of Polar Research (NIPR) is leading a six year prioritized project of the Antarctic research observations since 2010. One of the sub-projects is entitled "the global environmental change revealed through the Antarctic middle and upper atmosphere". Profiling dynamical parameters such as temperature and wind, as well as minor constituents is the key component of observations in this project, together with long-term observations using existent various instruments in Syowa, the Antarctic (39E, 69S). As one of the instruments in this project, a new resonance scattering lidar system with tunable wavelengths is developed to be installed and operated at the Syowa Station. The lidar transmitter is based on injection-seeded, pulsed alexandrite laser for 768-788 nm (fundamental wavelengths) and a second-harmonic generation (SHG) unit for 384-394 nm (second harmonic wavelengths). In order to tune the seeder laser to absolute Potassium resonance line, Doppler-free spectroscopy with a Potassium cell is crucial. The measurement was done at NIPR and the Doppler-free spectrum was recorded with 0.005 pm wavelength resolution. Three absorptions spaced with 0.05pm at the cross-over wavelength were clearly measured. In this talk, details of the experiment will be shown.

Keywords: Antarctica, lidar, Potassium, resonant scattering, Doppler Free

## Development of a 3D sodium lidar: synchronous experimentation and validation

MURANAKA, Wataru<sup>1\*</sup> ; KAWAHARA, Taku<sup>2</sup> ; NOZAWA, Satonori<sup>3</sup>

<sup>1</sup>GSI, Shinshu University, <sup>2</sup>Faculty of Engineering, Shinshu University, <sup>3</sup>STE Lab., Nagoya University

Shinshu University, Nagoya University and RIKEN developed an all solid-state, high-power Na lidar for the temperature/wind measurements in the MLT region over EISCAT radar site in Tromsø (69 N), Norway. Current observation is five-direction mode applied to the fixed direction such as vertical and 30 degree tilted to the north, south, east and west from the vertical.

We are now updating the lidar to multi-direction system which has never been done with resonant lidars. The transmission system uses two mirrors with electric rotary stages to emit laser light to any direction of the sky. Receiver system uses a telescope controlled by a PC. The coordination of the telescope is done with direction of some bright stars. This repeatability pointing to the same direction is 5.3 mrad.

In this talk, we will discuss the experimental results of the synchronized experiments with the laser direction and telescope field-of-view.

Keywords: sodium, lidar, three dimensional

## Analysis of the factors of seasonal variation of the thermosphere-mesosphere NO observed at Syowa Station

UEMURA, Miku<sup>1</sup> ; ISONO, Yasuko<sup>1</sup> ; MIZUNO, Akira<sup>1</sup> ; NAGAHAMA, Tomoo<sup>1</sup> ; EJIRI, Mitsumu K.<sup>2</sup> ; TSUTSUMI, Masaki<sup>2</sup> ; NAKAMURA, Takuji<sup>2\*</sup>

<sup>1</sup>Solar-Terrestrial Environment Laboratory, Nagoya University, <sup>2</sup>National Institute of Polar Research

When high-energy particles such as solar protons and energetic electrons fall down to the earth's atmosphere, the nitrogen oxides (NO, NO<sub>2</sub>) are increased in the mesosphere and the upper stratosphere in the polar regions (e.g. Lopez-Puertas et al. 2005). In collaboration with the National Institute of Polar Research, Nagoya University Solar-Terrestrial Environment Laboratory installed a millimeter-wave spectroscopic radiometer at Syowa Station in Antarctica. We have conducted continuous observation of the NO spectrum since January 2012. The NO column density derived from this observation shows a seasonal variation that the NO column density increases up to about  $1.7 \times 10^{15} \text{ cm}^{-2}$  in winter and decreases down to about  $0.5 \times 10^{15} \text{ cm}^{-2}$  in summer. In order to understand the mechanism of the seasonal variation, we compared it with seasonal variation of CO vertical distribution in thermosphere-mesosphere and the length of sunshine hours at Syowa Station. Since CO photochemical lifetime is longer than or equal to the horizontal and vertical transport in the thermosphere and the stratosphere, CO can be considered as a good tracer of atmospheric transport. We used CO data obtained by AULA / MLS (Version3.3).

The CO volume mixing ratio in a latitude range of 65 S-75 S and an altitude range of 0.1-0.01 hPa shows a tendency that the mixing ratio increased in winter and decreased in summer. The peak altitude of the mixing ratio changed from upper altitude to lower altitude during winter, suggesting downward transport of the atmosphere. The commencements of the increment of the NO column density and the CO mixing ratio were almost coincident, but the temporal variation patterns of NO and CO did not agree well with each other especially in the decrement phase. On the other hand, the temporal variation pattern of the NO column density and the length of night time showed good correlation throughout the period during which the NO enhancement was significant. Thus the variation of the NO column density in the lower thermosphere-mesosphere is considered to be caused by both the descending of the air mass and the photochemical process.

In this poster, we will present more detailed discussion on the relationship among the NO column density, CO mixing ratio, and length of the night time based on the dataset including the new data acquired this year.

Keywords: microwave spectroscopy, Nitric Oxide



## Small spatial scale field aligned currents in middle and low latitudes as observed by the CHAMP satellite

NAKANISHI, Kunihiro<sup>1\*</sup> ; IYEMORI, Toshihiko<sup>1</sup> ; AOYAMA, Tadashi<sup>1</sup> ; LUHR, Hermann<sup>2</sup>

<sup>1</sup>Department of Geophysics, Graduate School of Science, Kyoto University, <sup>2</sup>GeoForschungsZentrum, GFZ, Potsdam, Germany

The magnetic field observation by the CHAMP satellite shows the ubiquitous existence of small scale (1-5 nT) magnetic fluctuations with period around a few tens seconds along the satellites. From characteristics of the amplitude and period, they can be interpreted as the spatial structure of small scale field-aligned currents generated by the ionospheric dynamo driven by atmospheric gravity waves propagating from the lower atmosphere. The mechanism is the following; first, the gravity waves generated by the lower atmospheric disturbance propagate to the ionosphere; the neutral winds oscillate, cause ionospheric dynamo and Pedersen and Hall currents flow; because the dynamo region is finite, the currents cause polarized electric fields; and the polarized electric fields propagate along the geomagnetic field as Alfvén waves accompanied by field-aligned currents, at the same time, the ionospheric currents divert to the field aligned currents; finally the CHAMP satellite observes the spatial structure of the field aligned currents generated in this way as a temporal change along the path, because the temporal variation of the gravity waves are slow enough, i.e., more than a few minutes, that is, that of field aligned current can be ignored and nearly constant for the satellite crossing the currents.

This time we analyze correlation relation of the two components perpendicular to the geomagnetic field to find the following tendencies. About the magnetic data at the observed point, 1) if inclination and declination are plus and plus respectively, a correlation coefficient tends to be minus; 2) if inclination and declination are plus and minus respectively, it tends to be plus; 3) if inclination and declination are minus and plus respectively, it tends to be plus; 4) if inclination and declination are minus and minus respectively, it tends to be minus.

We report the model of the current system consistent to the characteristics of the magnetic fluctuations including the tendency of the correlation relation.

Keywords: spatial structure of field aligned currents, middle and low latitudes, the CHAMP satellite, atmospheric gravity wave, the lower atmospheric origin, correlation relation



## Atmospheric origin of small-scale magnetic fluctuations as observed by CHAMP above the ionosphere

AOYAMA, Tadashi<sup>1\*</sup> ; IYEMORI, Toshihiko<sup>2</sup> ; NAKANISHI, Kunihito<sup>1</sup>

<sup>1</sup>Graduate School of Science, Kyoto University, <sup>2</sup>Graduate School of Science, Kyoto University

We analyzed magnetic field data obtained by a LEO(Low Earth Orbit) satellite, CHAMP(altitude 300~450 km), and found out the global distribution of the short-period(10~40 s) and small-amplitude(0.1~5 nT) magnetic fluctuations in middle and low latitudes. We have reported that these fluctuations are small-scale structure(~100 km) of the field-aligned currents generated by dynamo action in the ionospheric E-layer and the dynamos are caused by the atmospheric gravity waves (horizontal scale is ~100 km) because of the characteristics of geographical and seasonal dependence of their amplitude.

In this paper, we focus on the mesoscale meteorological events to clarify the atmospheric origin such as typhoon which is possible to generate atmospheric gravity waves, and compare with magnetic fluctuations as observed by the CHAMP satellite above the ionosphere. We trace from the location of CHAMP to each footpoint in the E-layer along geomagnetic field line, and then compared with meteorological phenomena beneath the footpoint.

As a result, we detected large amplitudes of geomagnetic fluctuation above typhoons.

Keywords: field-aligned current, ionospheric dynamo, atmospheric gravity wave, acoustic resonance, CHAMP satellite, typhoon

## Optimization of notification system for bright meteor signals by using wide angle images at multiple sites

IYONO, Atsushi<sup>1\*</sup> ; WADA, Naoki<sup>2</sup>

<sup>1</sup>Dept. of Fundamental Science, Okayama university of Science, <sup>2</sup>Graduate School of Science, Okayama university of Science

### 1. Purpose and Background

The sky monitoring system by using wide angle images have been maintained until Nov. 2011 at Okayama University of Science. The CCD camera system provides the slow shutter images every 3 second, and they have been transferred simultaneously to data storage server via the Internet connection. This system enables to monitor the real time condition of the sky. In the obtained images, bright meteors and sometimes fire balls were registered. We have been developing our new system which can provide quick analysis results for meteor and fire ball at the moment of observations. In this report, we describe the new sensor systems of thermography and low frequency sounds to increase the detection efficiency of brighter meteors and fire balls.

### 2. System

In the sky monitor system, CCD camera with wide angle lens and image server system have been operated in 24 hours/day. The exposure of CCD cameras has been set to be 4 second. The acquired image data have been stored in PC system via the internet ftp command. 28,800 images(500MB data

size) are stored in each day. In offline mode, images are processed with contrast enhancement module, image differentiating and object detection module. To detect meteors and fire balls effectively, we activated the IR image sensors and low frequency sound sensors as well as imaging devices.

### 3. Development

Our purposes are that new analysis system for online processing of images, IR sensors and low frequency sensors have been developed in order to provide the information of the arrival of meteor and fireballs, arrival directions and brightness profiles. We are going to present new system and analysis result in this reports

Keywords: meteor, fireball, simultaneous? observation, meteor shower

## Measurement of propagation characteristics of MF band radio waves in lower ionosphere by S-310-40 sounding rocket

ISHISAKA, Keigo<sup>1\*</sup> ; ITAYA, Keita<sup>1</sup> ; ASHIHARA, Yuki<sup>2</sup> ; ABE, Takumi<sup>3</sup> ; ENDO, Ken<sup>4</sup> ; KUMAMOTO, Atsushi<sup>4</sup>

<sup>1</sup>Toyama Prefectural University, <sup>2</sup>NARA National College of Technology, <sup>3</sup>ISAS/JAXA, <sup>4</sup>Tohoku University

The ionospheric D region is important in radio wave propagation because it absorbs energy from waves at MF, HF and VHF, and it reflects LF and VLF signals. Then D region is present only during daylight hours. Therefore, in the night-time, the MF band radio waves are propagated as far as an area where its radio waves cannot be propagated in the daytime. This reason why the radio waves cannot receive is that the D region is disappeared at night. However, the MF band radio waves that transmit from distant place have not been often received at the mid latitude in the night-time. In this time the sporadic E region cannot be observed by the ionogram. We guess that the D region appear in the lowest ionosphere like a daytime. To farther study the structure of the lowest ionosphere, we propose a method to measure the very low electron densities that occur at altitudes from 50 km to 90 km using the partial and perfect reflection characteristics of electromagnetic waves.

S-310-40 sounding rocket experiment was carried out at Uchinoura Space Center (USC) at 23:48 JST on 19 December, 2011. The purpose of this experiment is the investigation of characteristics of radio wave propagation in the ionosphere and the estimation of electron density structure in the lower ionosphere, when the intensity of radio wave measured on the ground will be attenuate at night-time. In order to measure the radio waves, a LF/MF band radio receiver (LMR) is installed on the sounding rocket. The LMR has measured the propagation characteristics of four radio waves at frequencies of 60 kHz (JJY signal from Haganeyama radio station), 405 kHz (NDB station from Minami-Daito), 666 kHz (NHK Osaka broadcasting station) and 873 kHz (NHK Kumamoto broadcasting station) in the region from the ground to the lower ionosphere. The LMR consists of a loop antenna, a pre-amplifier and a detector circuit. The loop antenna is set up in the nose cone, which is transparent to the LF/MF band radio waves, and is not deployed during the flight. Therefore, the LMR can measure the relative attenuation of radio waves from the ground up to the ionosphere. Furthermore the loop antenna consists of three loop antennas in order to measure three components of four radio waves. Then we can obtain the propagation directions of radio waves in the ionosphere directly.

A propagation vector can be obtained from the propagation characteristic of radio wave. It is possible to estimate electron density profile from a propagation vector, because the propagation vector is dependent on the electron density profile in the radio wave propagation region. We have estimated the electron density profile by the propagation vector. When the electron density profile estimated by the propagation vector was compared with the electron density profile measured with the Langmuir probe and the impedance probe onboard the S-310-40 sounding rocket, it was found that electron density becomes the maximum at an altitude of 104 km.

We show the results of propagation characteristics of radio waves in the ionosphere and explain the propagation vector of radio wave in the ionosphere. And the electron density profile in the ionosphere can be estimated by the propagation vector. We will show the result that it is investigated the influence the lowest ionosphere region has on a MF band radio wave in this study.

Keywords: ionosphere, propagation characteristic of radio wave, rocket experiment

## Measurement of LF Standard-Frequency Waves JJY along the track of Shirase during JARE55: Preliminary Report

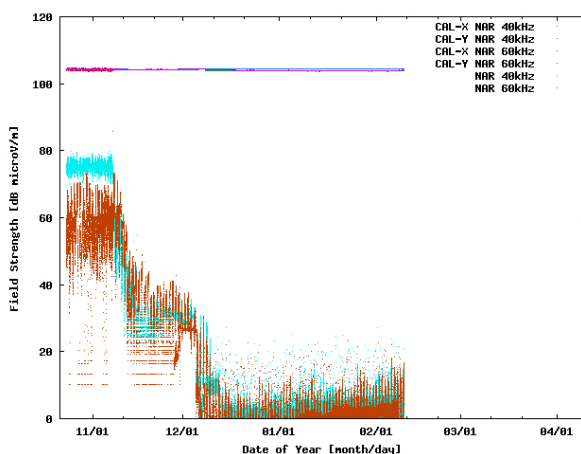
KITAUCHI, Hideaki<sup>1\*</sup> ; NOZAKI, Kenro<sup>1</sup> ; ITO, Hiroyuki<sup>1</sup> ; KONDO, Takumi<sup>1</sup> ; TSUCHIYA, Shigeru<sup>1</sup> ; IMAMURA, Kuniyasu<sup>1</sup> ; NAGATSUMA, Tsutomu<sup>1</sup>

<sup>1</sup>NICT

We developed a highly sensitive, reliable receiving system for the purpose of reception of low frequency (LF) radio waves. The system consists of digital lock-in amplifiers and crossed-loop antennas. Digital lock-in amplifier (DLA) employs phase-sensitive detection (PSD) of periodic signal multiplied by the input reference source of the known signal frequency. This makes it possible to realize very narrow bandpass filter around the reference frequency, detecting/measuring that of very weak signal even in noisy environment. The antenna, on the other hand, consists of orthogonally crossed, larger double loops (receivers  $R_X$ ,  $R_Y$ ) and smaller doubles (transmitters  $T_X$ ,  $T_Y$ ): the former receivers  $R_X$ ,  $R_Y$  receive LF radio signals of x-, y-components, the latter transmitters  $T_X$ ,  $T_Y$  transmit an instant, weak signal from each x-, y-component for self calibration purpose. The self calibration test is performed by transmitting a weak LF signal for an instant every an hour from the transmitter  $T_X$ ,  $T_Y$  respectively, and receiving this signal from the receivers  $R_X$ ,  $R_Y$  to obtain preassigned field strength. This test indicates if the receivers of the system are working properly and allows us to obtain reliable measurements.

We apply the receiving system to measure the field intensity and phase of the standard frequency and time signals (SFTS) JJY of LF 40 kHz and 60 kHz during the summer expedition of the 55th Japanese Antarctic Research Expedition (JARE), from November 2013 to April 2014. Figure 1 shows temporal evolution of the field intensities JJY 40 kHz (light blue dots) and 60 kHz (brown dots) as well as the self-calibrating radio signals. Our receiving system detects both the LF JJY radio signals even offshore Syowa Station, Antarctic, about 14,000 km away from those transmitting stations. Also the field intensities of the self calibration test show about a consistent preassigned value, assuring the measurements.

Keywords: low frequency (LF) radio waves, call sign JJY of 40 kHz and 60 kHz, standard frequency and time signals (SFTS), self calibration, Japanese Antarctic Research Expedition (JARE), Japanese Antarctic Research Icebreaker Shirase



## Velocity distribution of electrons generating plasma waves around the wake of an ionospheric sounding rocket

ENDO, Ken<sup>1\*</sup> ; KUMAMOTO, Atsushi<sup>1</sup> ; KATO, Yuto<sup>1</sup>

<sup>1</sup>Department of Geophysics, Graduate School of Science, Tohoku University

When a body moves in plasma at supersonic velocity, a rarefied plasma region called 'plasma wake' is formed behind the body. Wakes can develop behind a solar system body immersed in solar-wind plasma as well as behind spacecraft such as satellites and ionospheric sounding rockets. There are several studies which report plasma waves around the wakes of a satellite and of the moon. Although there are not so many studies which report plasma waves generated in association with the rocket wake, observational results from two rocket experiments performed in 1998 and 2012 have shown generation of plasma waves around the wake of a rocket. It is very important to reveal the generation process of plasma waves near the rocket wake for understanding the universal physics related to the interaction between streaming plasma and a non-magnetized body as well as for interpreting wave data obtained in rocket experiments more accurately.

Our analysis has revealed three kinds of plasma waves observed in the S-520-26 rocket experiment in 2012. They are likely to be electrostatic electron cyclotron harmonic (ESCH) waves, upper hybrid resonance (UHR) mode waves, and whistler mode waves. They have spin-phase dependence in characteristic manners. These results indicate that the plasma waves should be generated inhomogeneously around the rocket. We have performed numerical calculations of plasma dispersion relations by assuming anisotropic velocity distribution functions such as electron beam and temperature anisotropy. As a result, positive linear growth rates have been obtained in the wave number and frequency ranges of UHR mode waves and ESCH waves in addition to electrostatic whistler mode waves. Accordingly, there have to be electrons with some anisotropic velocity distribution functions which are equivalent to those we assumed in the calculations. However, we have to clarify what kind of velocity distribution can be generated around the actual wake through the interaction between a sounding rocket and ionospheric plasma.

Singh et al. (1987) has performed a one-dimensional simulation of plasma entering a void region from the two sides using a Vlasov-Poisson code. They have found counterstreaming electron beams in the very near wake. However, their study concentrates on electrons on the wake axis and does not indicate distribution functions in other areas. Besides, temperature anisotropy could not be treated in their simulation because it is performed in one dimension in velocity space.

In order to investigate inhomogeneity of electron distribution functions around the rocket wake, we are developing a Vlasov-Poisson code with one-dimensional space and two-dimensional velocity space, which is redesigned from the simulation code used in Singh et al. (1987). In this simulation, we deal with cases that electrons and ions are filling in a void space. The time evolution can be understood as spatial distribution along the wake axis. The direction of one-dimensional space is along the geomagnetic fields, along which electrons and ions can move easily. The size of space is 10 m, which is divided into 1024 grids in the calculation.

In this presentation, we clarify the frequency range and spatial distribution of the plasma waves around the wake based on the analyses of S-520-26 rocket experiment data. We also discuss the velocity distribution of the electrons which can generate the plasma waves as observed. In addition, we report initial results of our simulation for investigating the velocity distribution of electrons around the wake.

Keywords: ionosphere, sounding rocket, wake, plasma wave, Vlasov simulation

## Atmospheric Neutral Analyzer for mass-resolved velocity distribution measurements: Verification of mass analyzer

SHIMOYAMA, Manabu<sup>1\*</sup> ; HAYASHI, Ayuko<sup>1</sup> ; ITO, Fumihiko<sup>1</sup> ; HIRAHARA, Masafumi<sup>1</sup>

<sup>1</sup>STEL, Nagoya University

In order to understand the temporal and spatial variability of the ionosphere-thermosphere system, simultaneous measurements of the composition and density of the neutral atmosphere and the velocity distribution of individual species are essential. However, most conventional types of instruments for neutral atmosphere lack the simultaneous capability of measuring neutral atmospheric velocity and resolving neutral mass.

We have designed the Atmospheric Neutral Analyzer (ANA) instrument to measure the detailed, mass-resolved 2-dimensional velocity distribution of neutral species, from which the corresponding density, mass composition, bulk velocity and temperature were derived. In this presentation, we will report the results from laboratory experiments for the performance verification on the prototype of mass analyzer along with the detailed and overall design determined by numerical simulation.

Keywords: neutral upper atmosphere, velocity distribution function, mass analysis



## Observation of resonance scattering light of Lithium vapor under daytime and moonlight condition and neutral wind analysis

KIHARA, Daiki<sup>1\*</sup>; KAKINAMI, Yoshihiro<sup>1</sup>; YAMAMOTO, Masa-yuki<sup>1</sup>; WATANABE, Shigeto<sup>2</sup>; HARD, Lucas<sup>3</sup>; LARSEN, Miguel<sup>3</sup>; YAMAMOTO, Mamoru<sup>4</sup>; HABU, Hiroto<sup>5</sup>; ABE, Takumi<sup>5</sup>

<sup>1</sup>Kochi Univ. of Tech., <sup>2</sup>Hokkaido Univ., <sup>3</sup>Clemson Univ., <sup>4</sup>Kyoto Univ., <sup>5</sup>ISAS/JAXA

### 1. Introduction

For the purpose of measurement of neutral atmospheric wind in lower thermosphere, we observed resonance scattering light of sunlit Lithium vapor released from a sounding rocket in the evening thermosphere in 2007 (e.g. Yamamoto et al., 2008). At that time, we successfully measured thermospheric neutral wind profile between 110 km and 400 km. In 2012, we observed resonance scattering light of sunlit Lithium at dawn, and estimated lower thermospheric neutral wind between 76 km and 127 km.

On July 4, 2013, a U.S.-Japan collaborative rocket experiment to observe neutral wind profile in daytime lower thermosphere with Lithium release was carried out at WFF (Wallops Flight Facility), NASA. A rocket to operate chemical release of Lithium was launched at 10:31:40 EDT (14:31:40 UTC). The rocket launched to southeastern direction released Lithium vapor three times between at about 90 km and 130 km altitude during the upleg, at about 40 km horizontally away from a ground-based observation site in WFF. Here we tried to observe of Lithium clouds from the ground-based and airborne observations with collaboration of Kochi University of Technology (KUT) and Clemson University.

On July 20, 2013, a rocket experiment to observe neutral wind profile in moonlit lower thermosphere with Lithium release was carried out at USC (Uchinoura Space Center), Japan. The S-520-27 rocket to operate chemical release of Lithium was launched at 23:57:00 JST and released Lithium vapor three times between at about 80 km and 120 km altitude during the downleg under the almost full moon condition (Moon age was 12). Here we tried to observe of Lithium clouds from 3 ground-based sites and an airplane.

### 2. Observations

Airborne observation of Lithium cloud was carried out under a condition with the sun at the backward direction while it flew to north-northeast at about 10 km (33,000 feet) altitude and at about 300 km away from the ground site at the southeastern direction. An observation site was set in WFF on ground. In order to detect the Lithium clouds in daytime skies with good S/N ratio, digital cameras (Canon EOS Kiss X4, Nikon D90) with 2 nm band pass filters (BPF) at 671 nm wavelength were used for all digital cameras. We installed three digital cameras in the aircraft NASA-8 and set two digital cameras on the ground site. A video camera (Watec, WAT-120N) with a 12 nm BPF was also used in the aircraft and on ground, respectively.

The Lithium clouds under moonlight condition was observed by using digital cameras, Watec, and cooled EM-CCD (BITRAN BQ-87EM) with 2 nm and 12 nm BPF from the JAXA airplane Hisyo as well as three ground-based observation sites (USC, Tanegashima and Muroto).

### 3. Results

A Lithium cloud under daytime sky condition was observed for about 25 minutes from the aircraft. The released Lithium vapor formed red clouds along the rocket trajectory just after the release. Afterwards, the Lithium trails were spread into complex shapes by strong wind shear in the altitude. We successfully observed Lithium clouds by the airborne observation.

A Lithium cloud under moonlight sky condition was observed for about 90 seconds from the aircraft and two ground sites.

### 4. Summary

We successfully observed 2 chemical releases of Lithium from the aircrafts and ground sites on July, 2013, in daytime and midnight. We succeeded the detection of resonance scattering light of Lithium vapor under daytime and moonlight sky condition in lower thermosphere. Owing to this experiment, we confirmed that we can measure altitude profile of the neutral atmospheric wind in lower thermosphere at almost all local time by using the chemical release of Lithium.

In this paper, we will discuss that the observed emission intensity of the resonance scattering light of Lithium vapor under daytime and moonlight sky condition in lower thermosphere, obtained results of the S/N ratio, preliminary results and problems of the neutral atmospheric wind measurement in daytime lower thermosphere.

Keywords: sounding rocket, thermosphere, neutral wind, Lithium Ejection Systems, airborne observation



## Improvement of the method for estimating thermospheric temperature using small FPIs and evaluation of their temperatures

NAKAMURA, Yoshihiro<sup>1\*</sup> ; SHIOKAWA, Kazuo<sup>1</sup> ; OTSUKA, Yuichi<sup>1</sup> ; OYAMA, Shin-ichiro<sup>1</sup> ; NOZAWA, Satonori<sup>1</sup>

<sup>1</sup>Solar-Terrestrial Environment Laboratory, Nagoya University

Fabry-Perot interferometer (FPI) is an instrument that can measure the temperature and wind velocity of the thermosphere from the ground through observation of airglow emission at a wavelength of 630.0nm. The Solar-Terrestrial Environment Laboratory (STEL), Nagoya University, has five FPIs as parts of the Optical Mesosphere Thermosphere Imagers. Two of those FPIs, possessing a large aperture etalon (diameter: 116mm), were installed at Shigaraki, Japan in 2000 and in Tromsø, Norway, in 2009. The other three small FPIs, using 70-mm diameter etalons, were installed in Thailand, Indonesia, and Australia in 2010-2011. They use highly-sensitive cooled-CCD cameras with 1024-1024 pixels to obtain interference fringes. However, appropriate temperature has not been obtained from the interference fringes using these new small-aperture FPIs. In the present study we aimed to improve the procedure of temperature derivation using these small etalon FPIs, to evaluate the accuracy for obtained temperatures and to perform statistical analysis of the temperature data obtained for 2-3 years.

The FPIs scan the sky in north, south, east, and west directions repeatedly by rotating a light receiving mirror. We determined each center of the laser fringe and sky fringes for north, south, east, and west directions. Then we found that they are slightly a few pixels different depending on the mirror directions. This difference of fringe centers seems to be due to distortion of the optics body, which is caused by the motion of the heavy scanning mirror on top of the optics. Thus, we decided to determine the fringe center for each direction. After this revision, we could make a reliable temperature determination. In this presentation, we show these procedures of temperature derivation and relation between airglow intensity and standard deviations of obtained temperatures as accuracy of temperature derivation. We also discuss effects of the etalon gap drift due to changes in etalon temperature for accuracy of measured thermospheric temperatures and winds.

Keywords: Fabry Perot Interferometers, thermospheric temperature

## Statistical characteristics of MSTIDs observed by 630-nm airglow imager and HF-radar echoes at Paratunka, Russia

MINOURA, Takeshi<sup>1\*</sup> ; SUZUKI, Shin<sup>1</sup> ; SHIOKAWA, Kazuo<sup>1</sup> ; OTSUKA, Yuichi<sup>1</sup> ; NISHITANI, Nozomu<sup>1</sup> ; HOSOKAWA, Keisuke<sup>2</sup>

<sup>1</sup>Solar-Terrestrial Environment Laboratory, Nagoya University, <sup>2</sup>Department of Communication Engineering and Informatics, University of Electro-Communications

Medium-scale traveling ionospheric disturbances (MSTIDs), which typically have a horizontal scale of 100-500 km and a period of ~1 h, are frequently observed in the F region ionosphere at middle latitudes. To date, quite a few observations of MSTIDs have been carried out especially in the middle latitudes; they predominantly had a northwest-southeast, (northeast-southwest) frontal structure and propagated southwestward (northeastward) in the northern (southern) hemisphere, however their generation and propagation mechanisms are not clear yet. Suzuki et al. [2009] investigated two dimensional characteristics of a nighttime MSTID using the SuperDARN Hokkaido HF radar at Rikubetsu, (43.5 N, 143.6 E), Japan, and an OI 630-nm airglow imager located at Paratunka (53.0 N, 158.2 E), Russia, within the radar field of view (FOV). The Doppler velocities of MSTID echoes observed by the SuperDARN radar showed systematic polarity changes which were consistent with airglow intensity variations. The electric field estimated from the airglow and SuperDARN observations, however, seems to be improbable and the E-F coupling processes would be important to explain the inconsistency. We investigated statistical characteristics of nighttime MSTIDs. Based on the coordinated airglow and SuperDARN measurements from 2011 to 2013, we investigated the relation between the MSTID amplitudes in the 630-nm airglow intensity and the Doppler velocities of the FAI echoes associated with the MSTID pattern. This study may give an observational insight into the E-F coupling quantitatively.

In this presentation, we will report the statistics of the relation of the FAI echoes and airglow signatures of the observed MSTIDs (5 events), which showed spatially conjugation in the radar FOV.

Keywords: airglow imager, Hokkaido SuperDARN radar, MSTID

## Detection of ionospheric disturbances caused by the earthquake using HFD

TAKABOSHI, Kazuto<sup>1\*</sup> ; NAKATA, Hiroyuki<sup>1</sup> ; TAKANO, Toshiaki<sup>1</sup> ; TOMIZAWA, Ichiro<sup>2</sup>

<sup>1</sup>Graduate school of Engineering, Chiba University, <sup>2</sup>Center for Space Science and Radio Engineering, Univ. Electro-Comm

Many studies have reported that ionospheric disturbances occur after giant earthquakes. This is because the acoustic wave and/or atmospheric gravity wave are excited by the ground perturbations or tsunami. The HF Doppler observation is suitable for detection of ionospheric disturbances since this can observe ionospheric vertical drift from Doppler shift of radiowaves (5006 and 8006 kHz) transmitted from the Chofu campus of UEC. In this study, using Doppler shift data of 5006 kHz, ionospheric disturbances associated with earthquakes are detected. When Doppler shift is fluctuated intensely after propagation time of Rayleigh wave from the seismic center to the observation points, the fluctuation is determined as a disturbance associated with the earthquakes.

In 55 events of earthquakes ( $M \geq 6.0$ ) occurred around Japan since 2003, fluctuations by earthquakes are detected in 14 events and the smallest magnitude is 6.4. No fluctuation is detected in some larger earthquakes than M6.4. Since the ionosphere is unstable at night, received frequency is disturbed and it is hard to determine the fluctuations caused by earthquake. In addition, the observation points are not always located near the seismic centers. When earthquakes occur near observation points at the daytime, it is expected that the fluctuations caused by earthquakes are observed even if the magnitudes of the earthquakes is smaller than M6.4.

We also examined the relationship between direction of fault and fluctuations of HFD data. Most of the earthquakes in Japan are reverse fault type. Because a hanging wall slides up in this type of an earthquake, it is expected that initial perturbation of a sound wave excited by the hanging wall is upward. Actually, in most of the events Doppler shifts are negative, which means that the ionosphere moves upward. Next we examined a normal-fault-type earthquake (Fukushima hama-dori earthquake, 2011/4/11), in which a hanging wall slips down. In this event, the epicenter is located at the east of Fukushima prefecture. Doppler data of three observation points (Iitate, Sugadaira, Kiso) are examined. In Iitate observatory, which is the closest to the epicenter, Doppler data shows that ionosphere moved only upward. On the contrary, in the other two points, Doppler data shows that ionosphere moved downward first and then upward, or upward first and then downward. Therefore, fluctuations of ionosphere can not be determined only by a type of fault. More detailed analysis using the seismometer is necessary.

Keywords: ionosphere, HFD, earthquake, acoustic wave, atmospheric gravity wave, fault

## Observations of seismo-traveling ionospheric disturbance during the 2011 Tohoku earthquake using HF Doppler

CHOU, Min-yang<sup>1\*</sup> ; TSAI, Ho-fang<sup>1</sup> ; LIU, Jann-yenq<sup>2</sup>

<sup>1</sup>Department of Earth Science, National Cheng-Kung University, Taiwan, <sup>2</sup>Institute of Space Science, National Central University, Taiwan

This paper reports seismo-traveling ionospheric disturbances (STIDs) induced by the 11 March 2011 M9.0 Tohoku-oki earthquake and following pan-Pacific tsunami by two networks of HF (high-frequency) Doppler sounding systems in Japan and Taiwan. The Hilbert-Huang Transform (HHT) is applied to analyze Doppler frequency shifts (DFSs) detecting STIDs, while the time delay, circle, ray-tracing, and beam-forming methods are used to compute the propagation of the detected STIDs. Both STIDs induced by the Rayleigh waves and tsunami of the Tohoku-oki earthquake are detected and discussed.

Keywords: STIDs, Ionosphere, earthquake, tsunami

## Spectrum of the neutral atmospheric waves derived from a numerical simulation of an earthquake

SHIMIZU, Yuki<sup>1\*</sup> ; NAKATA, Hiroyuki<sup>1</sup> ; TAKANO, Toshiaki<sup>1</sup> ; MATSUMURA, Mitsuru<sup>2</sup>

<sup>1</sup>Grad. School of Eng. , Chiba Univ., <sup>2</sup>Center for Space Science and Radio Engineering, University of Electro-Communications

It is important to examine the ionospheric disturbances excited by earthquakes, since this contributes to monitoring tsunamis from satellites. There are many reports of ionospheric disturbances occurred by giant earthquakes, such as the 2011 off the Pacific coast of Tohoku Earthquake. But characteristics of atmospheric disturbances, connecting the ionospheric disturbances with the ground and the sea surface, is not clarified because broad observation of the atmosphere in high resolution is difficult. In this study, calculating the spectra from the temporal variations of neutral atmospheric waves determined by a numerical simulation, we derived the features of the propagation of the atmospheric waves.

In this simulation, two dimensional model is used. The atmospheric perturbation is created by a vertical velocity assuming an upward motion of the sea surface or ground surface. Calculating the temporal variations of neutral density, we derived their spectra.

As a result, it is shown that behavior of atmospheric waves is different for the frequency. For a notable example, variations around 1 mHz propagate to high altitudes 450 km ~500 km and long distance 800 km. On the other hand, variations around 10 mHz propagate almost the same distance in lower altitude of 300 km or less. In addition, variation at 4 mHz are located above the epicenter at 350 km. This causes the variation of GPS-TEC at 4 mHz associated with earthquakes that have ever been reported.

Keywords: ionosphere, earthquake, acoustic wave, gravity wave

## **Ionospheric effects on the F region during the Sunrise for the annular solar eclipse over Taiwan on 21 May 2012**

CHUO, Yu-jung<sup>1\*</sup>

<sup>1</sup>Department of Information Technology, Ling Tung University

On 21 May (20:56, Universal Time; UT, on 20 May), 2012, an annular solar eclipse occurred, beginning at sunrise over southeast China and moving through Japan, sweeping across the northern Pacific Ocean, and completing its passage over the western United States at sunset on 20 May (02:49 UT, 21 May), 2012. We investigated the eclipse area in Taiwan, using an ionosonde and global positioning system (GPS) satellites measurements. The measurements of foF2, hmF2, bottomside scale height around the peak height (Hm), and slab thickness (B0) were collected at the ionosonde station at Chung-Li Observatory. In addition, we calculated the total electron content (TEC) to study the differences inside and outside the eclipse area, using 3 receivers located at Marzhu (denoted as MATZ), Hsinchu (TNML), and Henchun (HENC). The results showed that the foF2 values gradually decreased when the annularity began and reached a minimum level of approximately 2.0 MHz at 06:30 LT. The hmF2 immediately decreased and then increased during the annular eclipse period. The TEC variations also appeared to deplete in the path of the eclipse and opposite to the outside passing area. Further, the rate of change of the TEC values (dTEC/dt measured for 15 min) was examined to study the wave-like fluctuations. The scale height near the F2 layer peak height (Hm) also decreased and then increased during the eclipse period. To address the effects of the annular eclipse in the topside and bottomside ionosphere, this study provides a discussion of the variations between the topside and bottomside ionospheric parameters during the eclipse period.

Keywords: ionospheric physics, ionospheric disturbances, solar radiation effects

## Horizontal shapes of mid-latitude sporadic-E observed with GPS-TEC

MAEDA, Jun<sup>1\*</sup> ; HEKI, Kosuke<sup>1</sup>

<sup>1</sup>Graduate school of Science, Hokkaido University.

The horizontal shapes of sporadic-E (Es) have remained uncovered due to the lack of effective observation methods. We use a dense array of Global Positioning System (GPS) receivers in Japan to map horizontal shapes of mid-latitude sporadic-E layers and explore their diversity. The spatial and temporal resolutions of the GPS array are ~25 km (in horizontal) and 30 s, respectively, which is ideal for studying the horizontal shape and movement of sporadic-E. Sporadic-E can be identified as positive anomalies of total electron content (TEC) along the line of sight between a satellite and a ground-based GPS station.

The results of GPS-TEC observation, i.e., mapping of positive TEC anomaly caused by mid-latitude sporadic E are presented in this presentation with a special emphasis on latitudinal and temporal variations of horizontal shapes of Es-layers. We analyzed ~100 Es events in 2010-2013 to examine the latitudinal dependence of Es frontal structures with three study areas at different latitudes near ionosondes, namely Sarobetsu (geographical latitude: 45.16 N), Kokubunji (35.71 N) and Yamagwa (31.20 N).

As a result, strong Es shares the large-scale frontal structure as a common shape regardless of the occurrence latitude and time (e.g., morning, afternoon, and the evening). The horizontal structures of large-scale fronts are typically elongated in east-west (E-W) with the length and width of ~300 km and ~30 km, respectively. However, lengths vary from 30 to 300 km by occasion. The alignment of frontal structures prefers E-W, ENE-WSW and NE-SW alignment with some exception of NW-SE and NNW-SSE aligned structures.

We will also discuss the possible mechanisms for formation, development, and movement of mid-latitude sporadic-E based on the results of our observations and proposed theories.

Keywords: Sporadic-E, GPS, TEC



## GPS-TEC observation using two-frequency software receiver

ASHIHARA, Yuki<sup>1\*</sup> ; KOMATSU, Kazuki<sup>1</sup>

<sup>1</sup>Dept. of Electrical Engineering, Nara National College of Technology

Global Positioning System (GPS) is a high accuracy positioning system that uses radio waves transmitted from several GPS satellites. The carrier signals of GPS satellites, there are two frequencies of L1 (1575.42MHz) and L2 (1227.60MHz). In the ionospheric plasma, the refractive index depends on the electron density. In addition, since the plasma is dispersive medium, each of L1 and L2 waves has different refractive indexes. Therefore, it is occurred propagation delay time (phase difference) in between these signals.

GPS-TEC (GPS Total Electron Contents) is a method to obtain the total electron contents along the line of satellite (LOS) from the phase difference between these signals. GPS-TEC is very useful technique to observe ionospheric electron density, but two-frequency GPS receiver is very expensive. Therefore, GPS-TEC has calculated by using GEONET data in most cases in Japan.

In the informatics and communication field, software receiver is being widely for demodulating the baseband signal, as a background of higher performance of computers. In this study, we build a software GPS receiver system, and receive the two-frequency signals. And we will evaluate the GPS-TEC data obtained by this observation.

Keywords: ionosphere, GPS-TEC, software receiver

## Total electron content observation by using GPS, QZSS and BeiDou

KINUGASA, Natsuki<sup>1\*</sup> ; TAKAHASHI, Fujinobu<sup>1</sup>

<sup>1</sup>Yokohama National University

There are several methods for observation of total electron content (TEC). TEC can be obtained from the measurement of global navigation satellite system (GNSS) such as GPS. Recently, RNSS (regional navigation satellite system) has been developed in China and Japan. We are trying to use RNSS for TEC observation.

RNSS makes TEC observation stable since a satellite is tracked continuously for long time. It is of benefit to study of plasmasphere because the altitude is higher than GNSS. There is also drawback. Since the direction of vector from ground receiver to satellite is not so variable, it is hard to observe the horizontal electron density distribution of ionosphere. This problem can be solved by combining with measurements of RNSS and GNSS. That is called multi-GNSS.

TEC can be calculated from the difference of delay between dual-frequency. The inter-frequency bias which remain in TEC measurement are required to estimated and removed. We will present model of ionospheric electron density distribution for the bias estimation procedure. We have constructed the observation system for GPS, Japanese QZSS, and Chinese BeiDou in Yokohama National University. Various observational results will be shown and discussed.

Keywords: TEC, QZSS, BeiDou, GPS, ionosphere, plasmasphere

## Total Electron Content prediction model over Japan using an artificial neural network

NISHIOKA, Michi<sup>1\*</sup> ; TSUGAWA, Takuya<sup>1</sup> ; MARUYAMA, Takashi<sup>1</sup> ; ISHII, Mamoru<sup>1</sup>

<sup>1</sup>National Institute of Information and Communications Technology

Forecasting Total Electron Content (TEC) is important for Space Weather; for predicting propagation delay of the radio waves in the ionosphere. Although several empirical and theoretical models have been developed, no model is available for forecasting TEC over Japan. Our purpose is to accomplish an operational TEC model over Japan using an artificial neural network (ANN) technique which is developed by Maruyama [2007]. In our model, absolute TEC values for each day from 27°N to 45°N in latitude and 127°E to 145°E in longitude were projected on a two-dimension TEC map, that is, a local-time and latitudinal map. Then the time-latitudinal variation was fitted by using the surface harmonic function. The coefficients of the expansions were modeled by using a neural network technique. For the learning process, we used absolute TEC value from 1997 to 2013. The input parameters are proxies of the season, the solar activity, and the geomagnetic activity. Thus, daily two-dimensional TEC maps can be obtained for any day when the input parameters are provided. We used input parameters which are available in real-time by some institutes and achieved one-day TEC prediction over Japan.

Keywords: Ionosphere, Total Electron Content, Operational model, artificial neural network

## Statistical Analyses of Ionospheric Storms Over 50 Years In Japan

NAKAMURA, Maho<sup>1\*</sup> ; KAMOGAWA, Masashi<sup>1</sup>

<sup>1</sup>Dpt. of Phys., Tokyo Gakugei Univ.

Statistical analyses of the ionospheric storms over Japan are carried out based on the long-term observations over 50 years in Japan. While there are many types of ionospheric variations such as ionospheric storms, plasma bubbles, TIDs and so on, ionospheric storms are most large fluctuations of electron density in the ionosphere. In general, the increase of the electron density is termed positive storm and the decrease of it is termed negative storm [1]. The positive storms cause satellite-positioning errors due to the delay of radio propagation and negative storms cause HF radio communication outages due to lowering the maximum usable frequency. Because these two types of ionospheric storms shows different characteristics on the duration, scale, and the seasonal dependences, we analyzed ionospheric storm occurrences using critical frequency of the F2 layer; foF2 obtained from ionograms over 4 observation sites (Wakkanai, Kokubunji, Yamagawa, and Okinawa) operated by National Institute of Information and Communications Technology, Japan (NICT) [2]. We extracted ionospheric storms based on the differences between the daily observation values and the one-month median in Japan for more than 50 years. Extracted storms of each station will be analyzed by the occurrences, duration, seasonal dependence and geomagnetic variations.

### References

- [1] G. W. Prokss, Ionospheric F-region storms, Vol. 2 of Hand book of Atmospheric Electro- dynamics, CRC Press, 1995.
- [2] World Data Center for Ionosphere, <http://wdc.nict.go.jp/>.

Keywords: ionospheric storms, critical frequency F2 layer, satellite navigation

## Statistical analysis of the Speckle applying the "Hinode" / XRT

YAMADA, Masanori<sup>1\*</sup> ; NOZAWA, Satoshi<sup>1</sup> ; SHIMIZU, Toshifumi<sup>2</sup>

<sup>1</sup>Graduate School of Science and Engineering, Ibaraki University, <sup>2</sup>Institute of Space and Astronautical Science, Japan Aerospace Exploration Agency (ISAS/JAXA)

" When a charge-coupled device (CCD) image is taken, white noise will appear identically main CCD image. For example, the trajectory of noise is watched like scar, small spot and snowstorm, which is called as spike, unwanted signal, and so on. In this study, noise is called " Speckle " . The speckle is due to the particle nature of photon when CCD is hit by Solar Energetic Particle(SEP) or cosmic ray. SEPs have high energy of 10 keV - 10 GeV, which are generated by solar flare, coronal mass ejection(CME). This reason is that SEP plays an important role in space weather. When SEPs with high energy of GeV order will come to earth magnetosphere, low earth orbit (LEO) satellite would be damaged the potential of single events like SEPs effect.

For this reason, this study analyzed Hinode / X-Ray Telescope (XRT) images and detected speckles. Analysis period is from January 2011 to July 2013. As a result speckles were periodic fluctuations and significantly increased, when on 00:04 UT March 7 2012, X5.4 Flare occurred.

Number of detected speckles had a time zone is 3 or 4 times as high as before the occurrence of the Flare. In addition periodic fluctuations are synchronized with orbital period. Moreover information of the satellite orbit indicates speckles increase over the High Latitude Zone (HLZ). Although this is suggested SEPs flow in HLZ, there is a region with high geomagnetic latitude, so speckles are caused by charged particles of non-SEPs.

This study reports on detailed consequence. Besides it looks at the correlations between decrease or increase in speckles and information of the satellite orbit or solar activity.

Keywords: Space Weather, SEP, Flare, CME, Hinode/X-Ray Telescope(XRT)

## Seasonal-longitudinal dependence of the occurrence of equatorial plasma bubbles observed by ISS-IMAP

TAKAHASHI, Akira<sup>1\*</sup> ; NAKATA, Hiroyuki<sup>1</sup> ; TAKANO, Toshiaki<sup>1</sup> ; SAITO, Akinori<sup>2</sup>

<sup>1</sup>Chiba University, <sup>2</sup>Kyoto University

Equatorial plasma bubbles (EPBs) are local depletions of the electron density in the ionosphere. Ionospheric irregularities are included in EPBs and cause radio signal scintillation. Recently, research on applying GNSS to Air Navigation System has progressed, therefore, it becomes more necessary to investigate the generation mechanism and the morphology of EPBs.

In this study, we analyzed seasonal-longitudinal dependence of the occurrence of EPBs using airglow-images obtained by ISS-IMAP (Ionosphere, Mesosphere, upper Atmosphere, and Plasmasphere mapping). In 630-nm airglow images, EPBs are visualized as black lines. 181 events are selected during 2012/09 - 2013/08. To calculate the longitudinal dependence of occurrence rate, we divide the ionosphere into 36 longitude bins, each 10 degrees wide. Since EPBs are observed at low and middle latitude, the total observation time is accumulated when  $|\text{latitude}| < 30$ . We calculate the occurrence rate as the number of EPBs detected over the total observation time.

The occurrence rate is high at the African-Atlantic-American regions in the equinoctial seasons. On the other hand, the occurrence rate is also high at American-Pacific regions in summer, which is not obtained in the previous study, Burke et al. [2004], in which EPBs are detected using plasma density data on DMSP satellite. The altitude of DMSP is 840 km, which is higher than the observation altitude of ISS-IMAP, that is about 250 km. Therefore, it is conceivable that the difference of occurrence rate of EPB is due to the altitude of the observations. This implies that ISS-IMAP observation could detect EPBs not developed to higher altitude.

Based on above, we will present seasonal-longitudinal variability of the Rayleigh-Taylor instability growth rate, contributing the development of EPBs using ionosphere model and other observational data.

Keywords: Equatorial ionosphere, Plasma bubble, airglow, ISS-IMAP